BEAM DYNAMICS CHALLENGES IN THE ESS LINAC

Yngve Inntjore Levinsen, M. Eshraqi, R. Miyamoto, M. Munoz, A. Ponton, R. De Prisco
European Spallation Source (ESS), Lund, Sweden

Abstract

The European Spallation Source (ESS) will be the world's brightest neutron source. It will be driven by a 5 MW proton linac that delivers a 2.86 ms pulse at 14 Hz, which means the peak beam power is 125 MW. This requires a careful design of the lattice structures, in order to allow for safe and reliable operation of the accelerator. We will discuss some of the design choices and some of the particular challenges that were faced during the design of the ESS lattice.

INTRODUCTION

The European Spallation Source ERIC project is already well into the construction phase [1], with an expected first beam on target in mid 2019. The long pulse spallation source is the first of its kind. The linear accelerator (linac) will provide an unprecedented proton beam power of 5 MW, with a proton beam current of 62.5 mA and a 2 GeV beam energy on target with a duty factor of 4 %. The linac is superconducting which allows for the long pulse length of 2.86 ms, and a 14 Hz pulse repetition rate.

The different sections of the ESS linac are listed in Table 1, and shown in Fig. 1. The normal conducting front-end consists of a ~2.5 m long LEBT after the ion source, followed by a ~4.55 m long 4-vane RFQ, a ~3.8 m long MEBT and 5 DTL tanks totalling ~39 m in length. There are three superconducting sections, first 13 spoke modules at the same radiofrequency as the normal conducting front-end of 352.21 MHz, then elliptical cavities at double the frequency. The two elliptical sections are called medium-β and high-β. A contingency space of 15 periods is left in for future upgrades. The total length of the accelerator including the transfer line is about 600 m.

Table 1: The Overview of the Different Sections of the ESS Linac

	Energy [MeV]	# modules	cav./mod. (Cells)	Length [m]
Source	0.075	-	0	-
LEBT	0.075	-	0	2.4
RFQ	3.65	1	1	4.6
MEBT	3.65	-	3	3.8
DTL	90.0	5	-	39
Spokes	216	13	2	56
Med.-β	571	9	4(6C)	77
High-β	2000	21	4(5C)	179
HEBT	2000	-	-	241

From a beam dynamics perspective, the main challenges associated with building such a high power linac are resulting from the high beam current. The result is strong space-charge forces which is challenging to accurately model and design for, and the low loss requirement of only 1 W/m means that an excellent control of the beam halo is required. Further, there is a high number of RF components that needs phase and amplitude corrections with beam. Due to the tight loss tolerances and need for high availability and reliability, there are tight requirements for dynamic errors of the RF phase and amplitude (with respect to the beam).

The design of the ESS lattice has been discussed in several earlier papers [1–6], including studies of the beam dynamics in individual sections as well as integrated studies [7, 8]. The design has undergone several changes since the TDR was released in 2012 [9]. The most significant change is that the beam energy has been reduced from 2.5 GeV to 2.0 GeV, while the beam current has been increased from 50 mA to 62.5 mA to keep the same 5 MW proton beam power at the target. The reduced space for accelerating structures has been converted to contingency space, so that the full upgrade to 3.5 GeV is still possible.

NORMAL CONDUCTING LINAC FRONT-END

The ion source is a microwave discharge ion source [10]. The source is designed to be able to provide a maximum of about 80 mA of proton beam current, with a pulse length flattop of up to 3 ms. The source voltage is 75 kV. The design choice is based on having a reliable high-current source with a long mean time between failures (MTBF). This is essential given the high reliability demands of a facility like ESS. The reliability of the ion source is expected to be very close to 100 %.

The low energy beam transport (LEBT) following the ion source consists of two solenoids of 330 mm length to focus the DC beam pulse, as well as a chopper and diagnostics to characterise the beam. The chopped beam is dumped on a cone aperture just before the RFQ entrance. A space-charge compensation of around 95 % is needed in order to meet the nominal performance.

The radio-frequency quadrupole (RFQ) is a 4-vane type with a length of 4.55 m. The RFQ is shown in simulations to have a very good beam capture, providing above 95 % of beam transmission through the structure under the assumption of a good space-charge compensation in the LEBT. The requirement is that at least 90 % of the beam should be transmitted through the RFQ. At the RFQ exit the beam energy has reached 3.62 MeV.

Between the RFQ and the drift tube linac (DTL), a matching is needed. This is done by the medium energy beam transport (MEBT), consisting of 11 quadrupoles and 3 RF buncher cavities. Additionally the head of the pulse coming from the LEBT will be degraded because there is a time

ISBN 978-3-95450-178-6

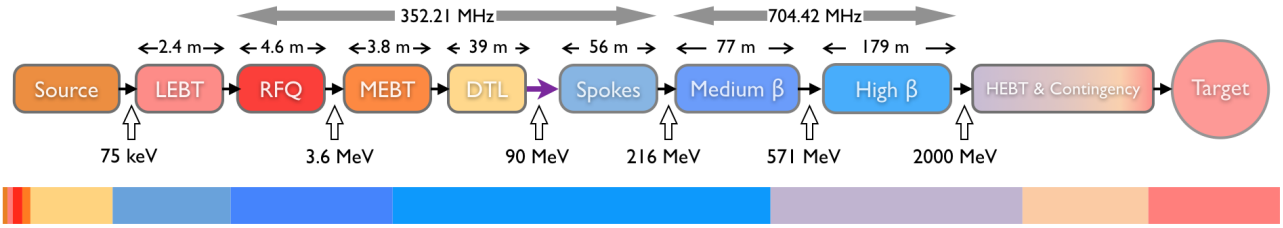

Figure 1: The layout of the ESS accelerator complex. The relative length of the sections are shown in the colour graph below. Superconducting sections are shown in shades of blue.

delay before the space-charge stabilises, so a chopper is installed in the MEBT to chop off the head and also the tail of the bunch with a faster rise time than the LEBT chopper. One steerer per quadrupole is available to correct the beam trajectory, and finally there is a selection of beam instrumentation to sufficiently characterise the beam coming out of the RFQ and assure we can do a proper matching into the DTL.

The ESS DTL consists of 5 tanks, accelerating the beam from 3.62 MeV to around 90 MeV. Permanent magnet quadrupoles (PMQ) in every second drift tube provide the transverse focusing. Steerers and BPMs are spread out in some of the empty drift tubes to correct and measure the trajectory. The BPMs are also used to measure the timing/phase of the beam, in order to correct the acceleration through the tanks. In between each tank there is a beam current monitor (BCT), and a Faraday cup is currently planned after tank 2 and 4. The first and foremost challenge in the DTL is to get a good beam transmission through the tanks, in particular in tank 1 where there is close to 0 transmission for non-ideal RF phases and amplitudes. Secondly it is important to steer the beam properly and provide a good quality beam towards the superconducting linac that follows.

SUPERCONDUCTING SECTIONS

The ESS linac consists of three families of superconducting cavities. The first are the double-spoke cavities, of which there are 13 pairs. The DTL and the spokes are separated by a low energy differential pumping section (LEDP). These cavities do not have as high accelerating gradient as the elliptical cavities, but allow for greater flexibility as the cavities can be retuned for different energies. That means we can retune the machine when a cavity is down with more ease, increasing reliability and availability of the machine.

In the rest of the ESS linac, the beam is accelerated by superconducting elliptical cavities. These cavities have a larger radial aperture and allow for a higher accelerating gradient, which is essential to reach the final target beam energy of 2 GeV within the approximately 350 m of acceleration structures. There are two families of elliptical accelerating cavities planned, with a contingency area following. The first structures are called medium-β, accelerating the beam from 216 MeV to about 571 MeV through 9 cryomodules of 4 six-cell cavities. After we have the high-β cavities which brings the energy to the nominal beam energy. The five-cell high-β cavities are almost the same length as the six-cell medium-β cavities, which allows the cryomodule to be the same length for both cavity types. We have 21 high-β cryomodules of 4 five-cell cavities in the ESS linac.

Each cryomodule houses a string of 2 (4) cavities in spoke (elliptical) sections. Each two ESS cryomodules are separated by what is called a linac warm unit (LWU). The LWU is composed of a quadrupole pair providing transversal focusing, a dual plane corrector, a dual plane BPM, as well as a central slot where there is space for beam diagnostics. The beam diagnostics in the linac is described in more detail in [11].

There is a trade off between lowering and increasing the RF frequency in superconducting structures. Lower frequencies are favoured due to looser tolerances in manufacturing cavity components. Lower frequencies also have the advantage of reducing RF losses in superconducting cavities, and ameliorating higher order mode (HOM) effects from the high-current beams. Higher frequencies are encouraged by the desire to keep the size of the superconducting cavities small, making them easier to handle and reducing manufacturing costs. The cryogenic envelope and power consumption are also reduced at higher frequencies [9].

The elliptical cavities run at twice the frequency of the upstream linac, 704.42 MHz. This frequency jump unfortunately provides a longitudinally unstable cross-over between the spoke cavities and the medium-β cavities, as will be shown later in this paper. The losses from this frequency jump are visible in the downstream linac until the dogleg.

In Fig. 2 we show the accelerating fields of the three families of superconducting RF cavities. The spoke cavity modules are shorter and provide lower accelerating gradient. We also see that the medium-β modules consist of 6 cells while the high-β modules consist of 5 cells at almost the same length.

LOSS DISTRIBUTIONS

For the ESS lattice it is important to have excellent knowledge of the expected loss levels in the machine. The machine will deliver 5 MW proton beam power, while the losses are required to stay below 1 W/m for the entire linac. That means that the relative amount of losses that can be accepted are on the order of 10^{-4}-10^{-7} per metre, depending on the beam energy where the losses happen.

Losses are seldom distributed evenly. Certain weaknesses in the lattice might produce more losses, or the misalign-

ISBN 978-3-95450-178-6

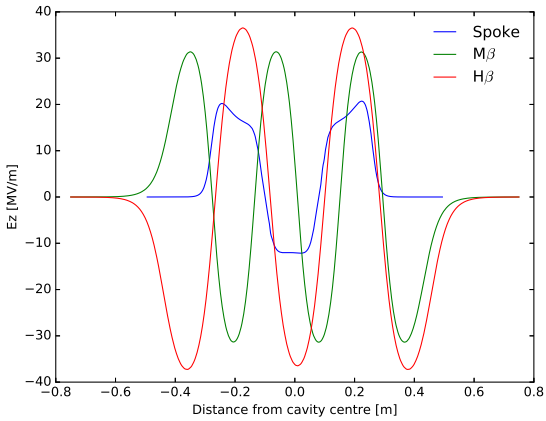

Figure 2: Comparison of the accelerating field in the three families of superconducting cavities. The double-spoke cavities shown in blue are followed by medium- and high-β cavities shown in green and red respectively.

ments are more unfavourable in certain regions. It is somewhat easier to predict loss distributions from a lattice than it is to predict the quantitative levels. There are also usually measures that may be taken until quantitative levels are mitigated, such as e.g. reducing the beam current.

We are here presenting a study of 20 000 machines with 600 000 macro-particles in each machine. For each machine we have applied the nominal tolerances for static and dynamic imperfections as have been defined earlier [7, 8]. In this study we have doubled the dynamic RF amplitude and phase jitters, in order to provoke more losses for the beam loss and activation studies. In the simulation we are therefore quoting the loss levels in arbitrary units, as a normalisation would represent losses that are significantly higher than what is actually expected in the machine. The increased dynamic error used does not change the distribution of losses significantly which makes this a useful way to improve statistics. Simulations are done from the exit of the RFQ until the beam reaches the target.

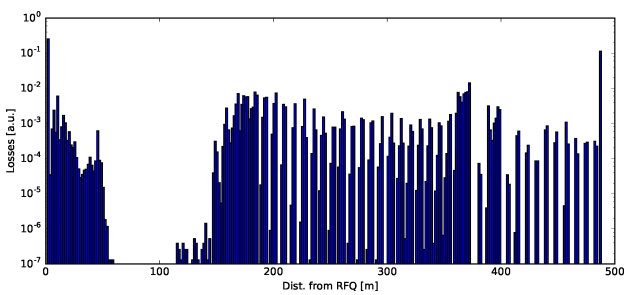

Figure 3: The distribution of losses along the ESS linac. The loss count is proportional to the number of particles lost. The last peak is in the dogleg. Losses in the last 10 m before target is excluded from the figure.

In Fig. 3 we show the losses along the linac, where the count is equal to the number of particles lost (i.e. no weight on the energy of the lost particles). We see a dense distribution of losses in the warm linac, a very clean spoke region and then losses from the medium-β onwards. The last peak at around 480 m is the beginning of the dogleg, where the off momentum particles are over steered into beam pipe.

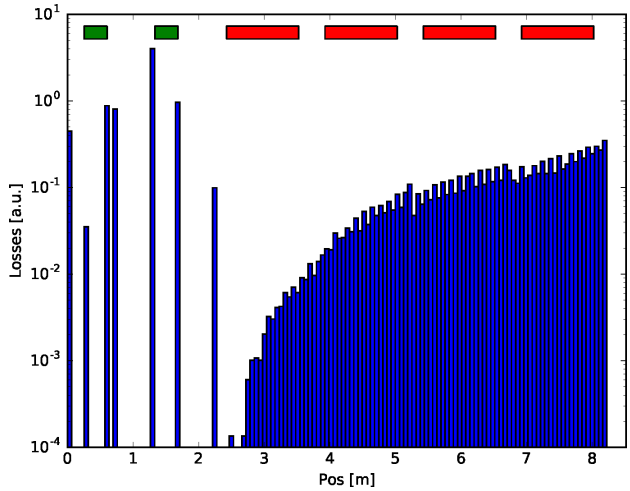

Figure 4: The distribution of the losses in a medium-β period. The LWU is contained in the first two metres, and the cryomodule in the next 6.5 m. The simulation has used a simplified aperture model where the LWU has 50 mm aperture and the cryomodule 60 mm aperture. Quadrupoles are marked in green, and cavities in red boxes.

There is an interesting regularity in the losses in the superconducting region which is shown better in Fig. 4. Here we show the loss distributions in each period of the medium-β overlapped. We see that the majority of the losses are in the warm linac (first 2 m of the figure), but there is a non-negligible amount of losses also inside the cryomodule. The relative amount of losses in the cryomodule may reduce with a more realistic aperture model, and would then be expected to be lost in the beginning of the downstream LWU.

In Fig. 5 the energy distribution of the losses in the medium-β and start of high-β is shown. We see here that there are very few losses being initiated from the normal conducting linac and the spoke section. The majority of losses have an energy equal to the medium-β input energy of 216 MeV or more. This is expected to originate from the challenging frequency jump between the spoke and medium-β section. We further note that there are almost no losses from the second half of the region these data are taken from, indicating that these are slow (longitudinal) losses.

In Fig. 6 the similar distribution is shown for the dogleg. Here the beam energy is 2 GeV, and we see that the dispersive region of the dogleg is cleaning some of the halo which is far from the reference beam energy. Also here we see losses from the frequency jump, with a logarithmically decaying number of particle lost as a function of particle energy.

ISBN 978-3-95450-178-6

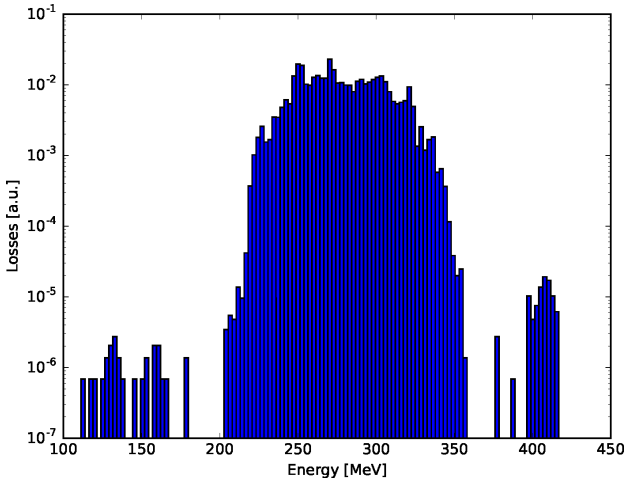

Figure 5: The energy distribution of the particles lost from the start of the medium-β and a few periods into the high-β section. Almost no losses from the upstream linac are seen.

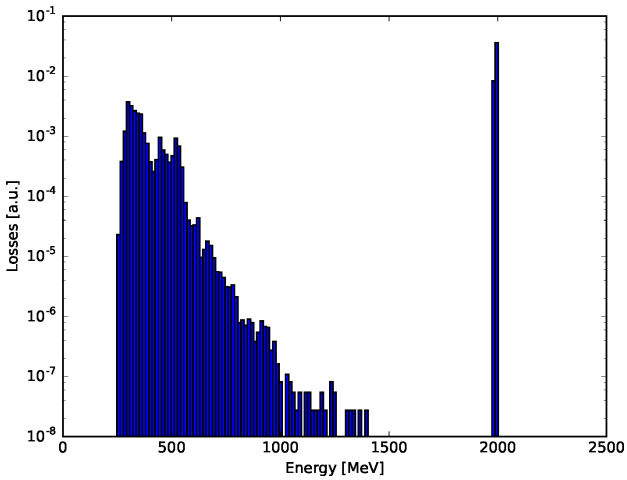

Figure 6: The energy distribution of losses in the dogleg region.

SUMMARY

The primary beam dynamics challenges of the ESS linac are following from the requirements of very low halo production and low fractional losses, in combination with a high current beam that produce strong space-charge forces in particular in the low energy front-end. Each section has been carefully designed and optimised with this in mind. In this paper we have discussed in more details the challenging frequency jump between the spokes and the medium-β sections, and shown that a significant part of the remaining simulated losses in the high energy part of the linac originates from this location.

REFERENCES

[1] M. Lindroos et al. 'ESS Progressing into Construction'. In: *IPAC'16, Busan, South Korea*. June 2016. DOI: 10.18429/JACoW-IPAC2016-FRYAA02.

[2] M. Lindroos et al. 'The European Spallation Source'. In: *Nuclear Instruments and Methods in Physics Research Section B: Beam Interactions with Materials and Atoms* 269.24 (Dec. 2011), pp. 3258–3260. ISSN: 0168583X. DOI: 10.1016/j.nimb.2011.04.012.

[3] R. Miyamoto et al. 'Beam Physics Design of the ESS Medium Energy Beam Transport'. In: *IPAC'14 Dresden, Germany*. 2014. DOI: 10.18429/JACoW-IPAC2014-THPME045.

[4] A. Ponton et al. 'ESS Normal Conducting Linac Status and Plans'. In: *LINAC'14, Switzerland*. 2014. http://jacow.org/linac2014/papers/thpp044.pdf

[5] Y. I. Levinsen et al. 'European Spallation Source Lattice Design Status'. In: *IPAC'15, Richmond, USA*. June 2015. DOI: 10.18429/JACoW-IPAC2015-THPF092.

[6] M. Eshraqi et al. 'ESS Linac Beam Physics Design Update'. In: *IPAC'16, Busan, South Korea*. 2016. DOI: 10.18429/JACoW-IPAC2016-MOPOY045.

[7] M. Eshraqi et al. *End to End Beam Dynamics of the ESS Linac*. 2012. https://cds.cern.ch/record/1558345

[8] M. Eshraqi et al. 'Statistical Error Studies in the ESS Linac'. In: *IPAC'14 Dresden, Germany*. 2014. DOI: 10.18429/JACoW-IPAC2014-THPME044.

[9] *ESS Technical Design Report*. 27th June 2013. http://docdb01.esss.lu.se/cgi-bin/public/DocDB/ShowDocument?docid=274

[10] L. Neri et al. 'Improved design of proton source and low energy beam transport line for European Spallation Source'. In: *Review of Scientific Instruments* 85.2 (1st Feb. 2014), 02A723. ISSN: 0034-6748, 1089-7623. DOI: 10.1063/1.4832135.

[11] A. Jansson, M. Eshraqi and S. Molloy. 'Beam Diagnostics for ESS Commissioning and Early Operation'. In: *IPAC'16, Busan, South Korea*. June 2016. DOI: 10.18429/JACoW-IPAC2016-MOPMR020.

ISBN 978-3-95450-178-6